MgO at high temperatures and pressures: shell-model lattice dynamics and molecular dynamics

1994 J. Phys.: Condens. Matter 6 393

(http://iopscience.iop.org/0953-8984/6/2/011)

J. Phys.: Condens. Matter 6 (1994) 393–404. Printed in the UK

MgO at high temperatures and pressures: shell-model lattice dynamics and molecular dynamics

David Fincham†‡, W C Mackrodt§ and P J Mitchell‡¶

† SERC Daresbury Laboratory, Warrington WA4 4AD, UK

‡ Department of Physics, Keele University, Staffordshire ST5 5BG, UK

§ ICI Chemicals and Polymers, The Heath, Runcorn, Cheshire WA7 4QD, UK

Received 23 August 1993

Abstract. MgO at high temperatures and pressures is studied by means of lattice dynamics in the quasi-harmonic approximation, and by molecular-dynamics simulation. The shell model is used to represent the polarizability of the oxygen ion. The two methods give very similar predictions for thermal expansion. However, the lattice dynamics fails at temperatures above 1500 K at atmospheric pressure, though not at high pressure (100 GPa). The predicted thermal expansion, using the Stoneham–Sangster and Lewis–Catlow potentials, is less than that observed experimentally. Predicted volumes at high pressure are too large. Shell-model molecular-dynamics simulation can be used to study the dynamics at temperatures close to the melting point. A small anharmonic shift of vibrational frequencies is observed.

1. Introduction

MgO (periclase) is an important mineral phase of the earth's lower mantle, and its properties at elevated temperatures and pressures are of great interest to the geophysicist. The ultimate theoretical challenge is to be able to make reliable estimates of the properties of this and other minerals, in regions of the phase diagram inaccessible to experiment, from first principles. Such calculations are not yet routine. An alternative approach adopts atomistic simulation methods based on the use of inter-atomic potential models [1]. Traditionally the models have been parameterized by fitting to experimental data such as lattice constants and elastic constants, though there is increasing interest in the use of theoretical methods in the development of potentials [2, 3]. For ionic materials the potential models often incorporate polarizability by means of the shell model [4]. The ion is represented by a core and a shell, both carrying charges, and linked by a harmonic spring. The shell is taken to be massless, and non-Coulombic interactions between ions are carried by the shells.

MgO at high temperatures and pressures has been studied by simulation by several authors. It adopts the rock-salt structure at all pressures considered here. Allan *et al* [4] compared results from a theoretically derived shell-model potential with those from a purely empirical potential. They used the method of lattice dynamics within the quasi-harmonic approximation [6], which enables thermodynamic functions to be calculated over a wide range of temperatures and pressures. The method incorporates quantum effects, in particular the zero-point vibrations, which may be important at low temperatures (the Debye temperature is 940 K). However, true anharmonic effects are not represented and the

¶ Present address: Department of Chemistry, University of Surrey, Guildford GU2 5XH, UK.

0953-8984/94/020393+12$07.50

quasi-harmonic approximation breaks down at the larger interionic separations that occur as the temperature approaches the melting point.

Molecular-dynamics simulations of MgO at high temperatures and pressure have been performed by Matsui [7]. In molecular dynamics forces are calculated directly from the potential function and full anharmonic effects are automatically included. Conventional molecular dynamics involves a purely classical simulation, though the work of Matsui [7] includes quantum corrections to order h^2. However, this model did not include ionic polarizability, which radically affects many properties, particularly vibrational frequencies.

Recently two of the present authors have developed [8] a simple and computationally efficient procedure for incorporating the shell model of ionic polarizability into molecular-dynamics simulations. This opens the way to the study of ionic materials without the limitations imposed by the use of either the rigid-ion model or the quasi-harmonic approximation. In this paper we apply the method to the study of MgO at high temperatures and pressures, looking particularly at thermal expansion and vibrational frequencies. The main aim is compare the predictions of molecular dynamics with those of lattice dynamics, and to extend these predictions to higher temperatures. We also investigate sensitivity to potential parameters by comparing results from two different empirical models. In addition, we look at the effects of the inclusion of polarizability in the interaction model.

2. Method

We use the very similar shell-model potentials of Stoneham and Sangster (SS) [9] and Lewis and Catlow (LC) [10]. These are ionic models in which the Mg^{2+} and O^{2-} ions are taken to have full charges. The non-Coulombic part of the potential has the usual form $A\exp(-r/\rho) - C/r^6$ and in both cases $A_{++} = C_{++} = C_{+-} = 0$, $A_{--} = 22\,764.4$ eV, $\rho_{--} = 0.1490$ Å and $C_{--} = 20.37$ eV Å^6. The potential models differ in the Mg–O interaction, with SS having $A_{+-} = 1346.6$ eV and $\rho_{+-} = 0.2984$ Å, while LC has $A_{+-} = 821.6$ eV and $\rho_{+-} = 0.3242$ Å. The MgO potential functions are illustrated in figure 1. The lattice spacing under standard conditions is 2.106 Å, and in this region the two curves are very close. They differ significantly at short separations, with the LC potential being the softer of the two. In both models the Mg^{2+} ion is non-polarizable, but the shell parameters y (shell charge) and k (core–shell spring constant) for the O^{2-} ion differ between the two models. SS have $y = -2.9345|e|$ and $k = 51.71$ eV Å^{-2}, while LC have $y = -2.0000|e|$ and $k = 15.74$ eV Å^{-2}. This results in the LC model having a larger polarizability than the SS model, $\alpha/4\pi\varepsilon_0 = 3.66$ Å^3 compared with 2.40 Å^3.

The lattice-dynamical calculations are carried out within the quasi-harmonic approximation. The Helmholtz free energy, $A(V, T)$, at a given volume and temperature is determined by the static lattice energy, E_L, and the classical vibrational frequencies $\nu_j(k)$, which are populated according to quantum statistics and integrated over the Brillouin zone. A is given by

$$A = E_L + \sum_{k,j}\left\{\tfrac{1}{2}\beta_j(k) + \ln\left[1 - \exp\left(-\beta_j(k)\right)\right]\right\} \tag{1}$$

where

$$\beta_j(k) = h\nu_j(k)/k_B T. \tag{2}$$

The pressure, p, and entropy, S, are given by

$$p = -(\partial A/\partial V)_T \tag{3}$$

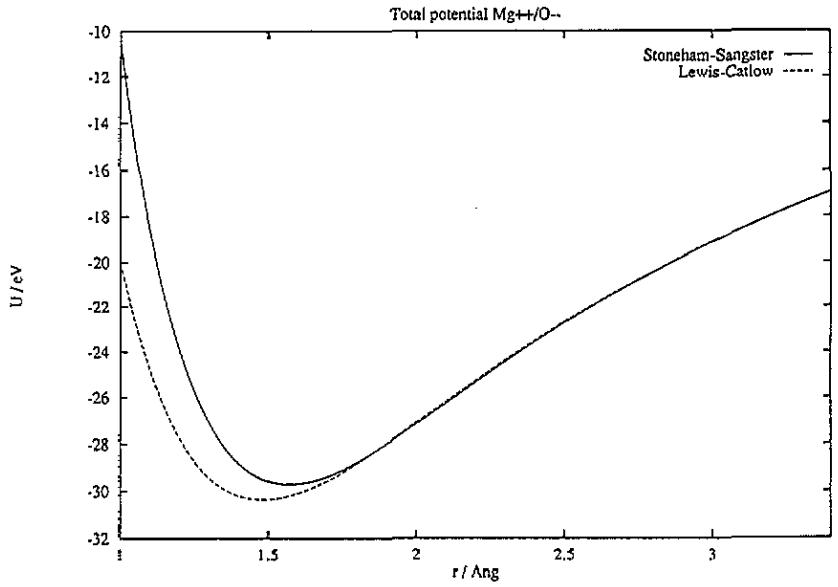

Figure 1. Mg–O interaction potentials in the models of Stoneham and Sangster [9] and Lewis and Catlow [10]. Curves shown are total potentials including Coulombic and non-Coulombic terms, without allowing for polarization.

and

$$S = -(\partial A/\partial T)_V = k_B \sum_{k,j} \{\beta_j(k)[\exp(\beta_j(k)) - 1]^{-1} + \ln[1 - \exp(-\beta_j(k))]\}. \tag{4}$$

Further details, including the integration over the Brillouin zone, may be found in [5].

The molecular-dynamics simulations use the adiabatic method for handling polarizable ions as described in [8]. In this method the shells are given a small mass and their motions, like those of the cores, are integrated by standard techniques. Appropriate choice of the shell mass ensures that the frequencies of the core–shell springs are well above the vibrational frequencies of the lattice and in these circumstances results are equivalent to those obtained with massless shells. In other respects the simulations are conventional. Systems of 216 ions were simulated within periodic boundaries with Coulombic interactions handled by means of the Ewald sum. Volumes were determined by carrying out simulations at constant pressure and temperature. These measurements are very accurate. Usually we re-equilibrated at the required temperature and pressure for 2 ps and then measured temperature, pressure and volume over a further 2 ps. Typically the actual temperature differed from the required temperature by less than 1 K, the actual pressure differed from the required pressure by less than 1 MPa, and the standard error in the volume was less than 0.001 $cm^3\ mol^{-1}$. Details of the program used are given in [11]. An explanation of our method of pressure calculation within the shell model is given in the appendix.

3. Results

Figure 2 shows the volume thermal expansion at atmospheric pressure. Results are presented as a ratio to the value at 300 K, V_0. There is close agreement between the results from

lattice dynamics (LD) and from molecular dynamics (MD) at temperatures up to 1500 K, validating the two methods and showing that the quasi-harmonic approximation works well up to this temperature. At higher temperatures the volumes predicted by lattice dynamics increase more rapidly, and this increase becomes catastrophic at around 2700 K. Comparing the MD results for the two potentials it can be seen that the LC potential shows a greater expansion than the SS potential. As well as the shell-model MD simulations, we have performed rigid-ion simulations using potentials that are otherwise identical. The figure shows that the polarizability reduces the rate of expansion, and that this effect is greater for the LC potential, which has the greater polarizability for the oxygen ion. Comparing with experimental results for the thermal expansion, it is clear that both potential models underestimate the expansion coefficient.

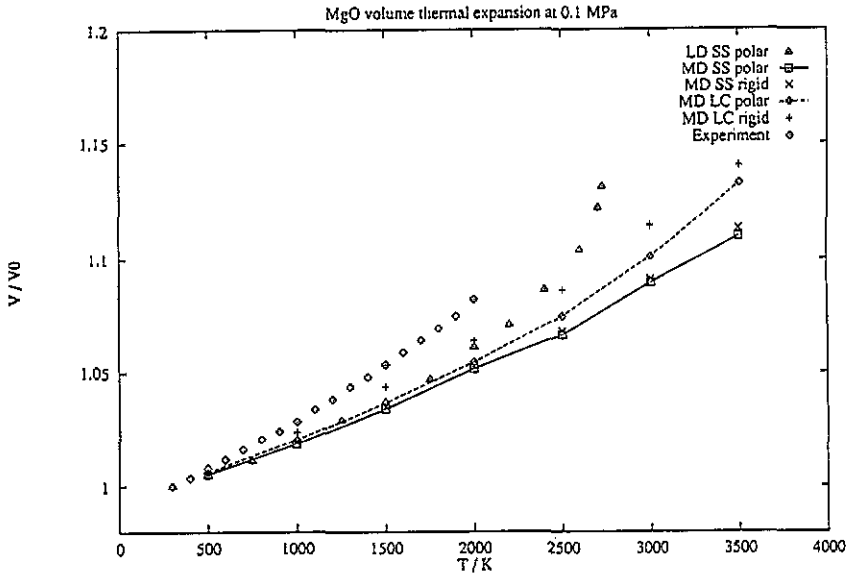

Figure 2. Volume thermal expansion at a pressure of 0.1 MPa, comparing results from lattice dynamics (LD) and molecular dynamics (MD), using the Stoneham–Sangster (SS) and Lewis–Catlow (LC) potentials. The experimental results are from [12]. Points marked 'polar' are shell-model simulations: those marked 'rigid' are rigid-ion simulations.

Table 1. Molar volumes and lattice parameters at 300 K.

	V_0 (cm^3)	a (Å)
LD SS polar	11.48	4.240
MD SS polar	11.44	4.236
MD SS rigid	11.45	4.236
MD LC polar	11.40	4.230
MD LC rigid	11.42	4.234
Experiment	11.24	4.212

Table 1 shows the values of V_0 and corresponding lattice parameters. In the MD results all models give very similar volumes, but these are rather larger than the experimental

values, which is surprising at first sight since the models are fitted to experimental data. There are two reasons for this discrepancy. First, models are often parameterized to have their energy minimum at the 300 K lattice spacing; they will therefore give a larger 300 K volume because of thermal expansion between 0 K and 300 K. The second contribution to the discrepancy arises from cut-off effects. The MD program adopts the usual approach of applying a spherical cut-off to the non-Coulombic forces at a radius equal to half the side of the computational box: 1.5 lattice parameters in our case. Potential fitting programs often apply a cut-off at much shorter distances, so as to include interactions up to next-nearest neighbours only. We have confirmed the fact that this effect can lead to discrepancies of the magnitudes shown in the table by using an energy minimization program to determine the equilibrium lattice parameter of the SS model. With a cut-off of $1.5a$ we find a lattice parameter a of 4.226 Å, but the use of a cut-off which excludes all interactions beyond next-nearest neighbours gives a lattice parameter of 4.216 Å. The increase in spacing with increase in cut-off is primarily due to the repulsions between third- and fourth-nearest neighbours, which have a larger effect than the attractive but rather weak oxygen–oxygen dispersion forces in these models. Running the MD program at 0 K confirmed the values from the energy minimization program. The LD results were obtained using the same cut-off as in the MD, but also include zero-point effects, giving a slightly larger volume. The magnitude of this effect is consistent with the estimate made by Matsui [7] of 0.05 $cm^3\ mol^{-1}$ for the quantum correction to the volume at 300 K.

The MD results are continued beyond the experimental melting temperature (around 3100 K) and in fact the simulations do not melt until the temperature reaches about 4500 K. This is because of superheating due to stabilization by the periodic boundaries. A future paper will discuss the estimation of thermodynamic melting temperatures in more detail: preliminary estimates suggest that the rigid SS model melts at around 4200 K and the rigid LC model at around 3400 K.

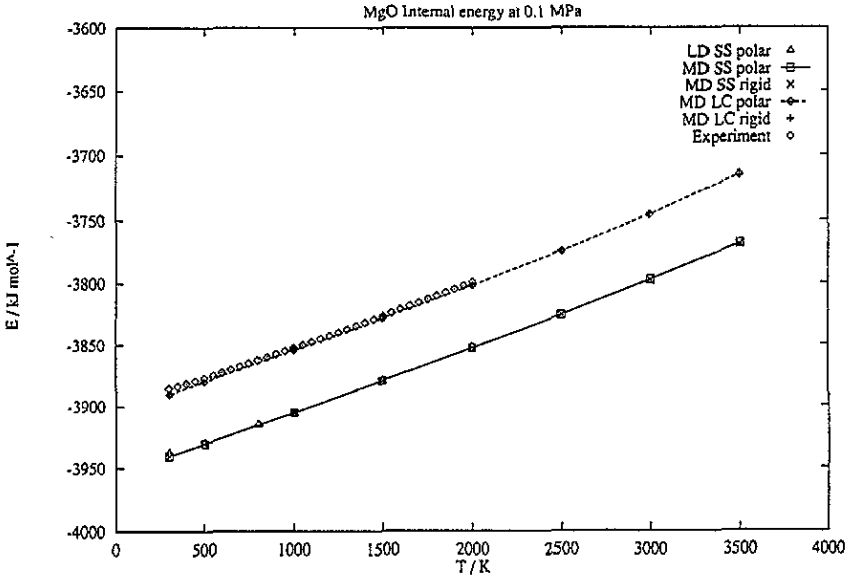

Figure 3. Internal energy as a function of temperature at a pressure of 0.1 MPa. The experimental values were obtained by integrating the specific-heat data from [12] and combining with the cohesive energy of 40.4 eV from standard tables.

Figure 3 shows the internal energy as a function of temperature. For the SS potential the LD results are in excellent agreement with the MD results. There is no detectable difference between results with and without polarization. This is to be expected as the oxygen site is centro-symmetric and the average polarization is zero. The results of the LC potential are in excellent agreement with experiment: the SS potential has an internal energy about 50 kJ mol^{-1} lower. This is due to the very slight difference between the two Mg–O potentials in the region of the lattice spacing, which can be seen in figure 1.

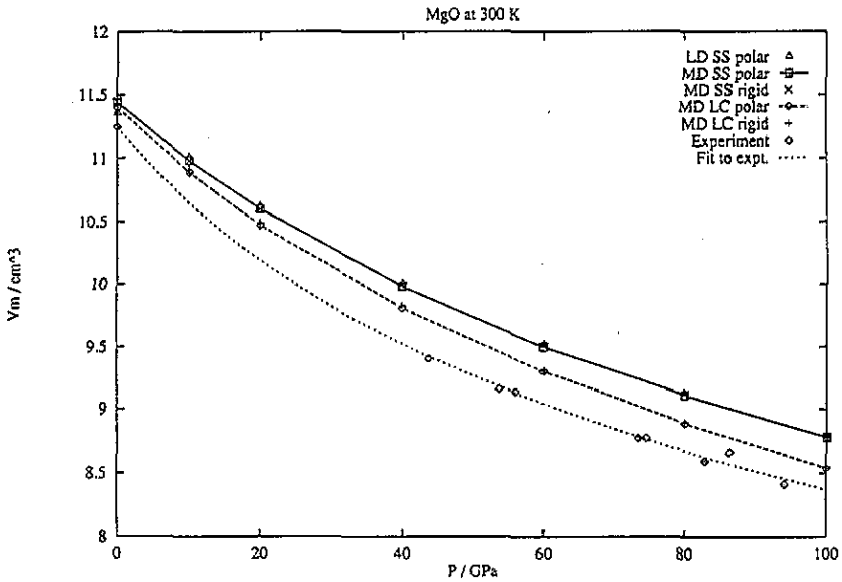

Figure 4. Volume as a function of pressure at 300 K. Experimental data are from [13].

Figure 4 shows the effect of compressing the system at 300 K. The LD results for the SS potential show volumes in almost exact agreement with the MD results. As expected, the LC model is more compressible than the SS model, but its compressibility at low pressures is still too small compared with the experimental data. Again, the inclusion of ionic polarizability has no effect on the results.

Figure 5 shows the thermal expansion at 100 GPa pressure. The LD volumes are slightly greater than the MD volumes. At these pressures and corresponding lattice spacings the LD can be continued up to higher temperatures. The introduction of ionic polarizability has an even more noticeable effect on reducing the expansion coefficient than at atmospheric pressure. The coefficient of thermal expansion is much lower at high pressures than at atmospheric pressure; this is discussed in detail in [5].

As already mentioned, the introduction of polarizability into models for ionic interactions is essential to reproduce vibrational frequencies. In MgO, for example, it reduces the LO frequency from around 30 THz to around 20 THz. Our previous paper [8] showed that shell-model MD gives frequencies in exact agreement with LD at 300 K. MD, however, is the only technique that permits the study of dynamical properties at high temperatures taking fully into account the anharmonic effects. To study these effects we chose to carry out simulations using the LC shell model. The simulations were at 3000 K, and a molar volume of 12.53 cm^3, which corresponds to zero pressure for this model. Two simulations were

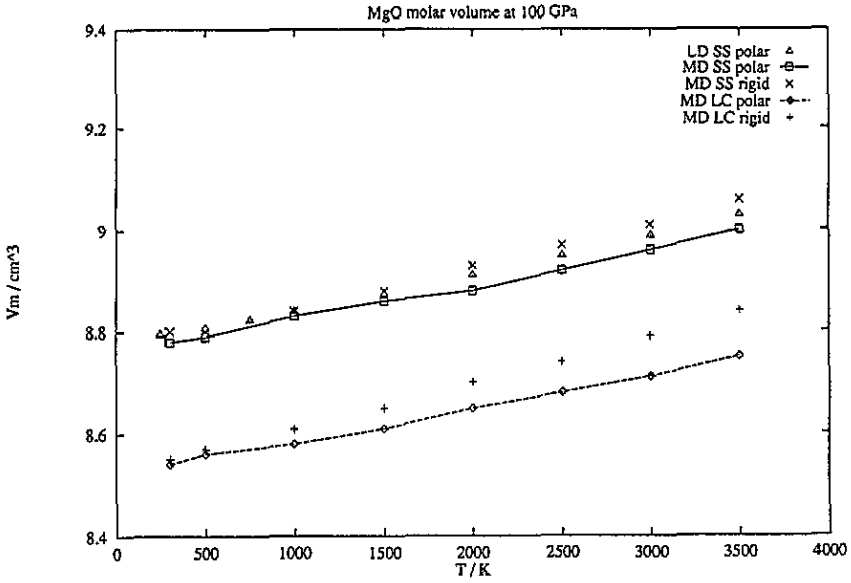

Figure 5. Thermal expansion at a pressure of 100 GPa.

performed, containing $3 \times 3 \times 3$ and $5 \times 5 \times 5$ unit cells respectively (216 and 1000 ions). This increases the number of k points that can be included in the analysis, since in any one simulation only those k values that are consistent with the periodic boundaries are accessible. Simulations were run for 10 ps.

The analysis of the MD trajectories was carried out in terms of current correlation functions. Specifically, if

$$j_k^{\mathrm{P}} = \sum_i v_i \exp(-\mathrm{i}\boldsymbol{k} \cdot \boldsymbol{r}_i) \tag{5a}$$

is the k-space component of the particle current, and

$$j_k^{\mathrm{Q}} = \sum_i q_i v_i \exp(-\mathrm{i}\boldsymbol{k} \cdot \boldsymbol{r}_i) \tag{5b}$$

is the k-space component of the charge current, we calculate the following four correlation functions: the transverse particle–particle current correlation

$$C_{\mathrm{PP}}^{\mathrm{T}}(k, t) = \langle \boldsymbol{k} \times j_k^{\mathrm{P}}(t) \cdot \boldsymbol{k} \times j_k^{\mathrm{P}}(0)^* \rangle \tag{6a}$$

the longitudinal particle–particle current correlation

$$C_{\mathrm{PP}}^{\mathrm{L}}(k, t) = \langle \boldsymbol{k} \cdot j_k^{\mathrm{P}}(t) \boldsymbol{k} \cdot j_k^{\mathrm{P}}(0)^* \rangle \tag{6b}$$

the transverse charge–charge current correlation

$$C_{\mathrm{QQ}}^{\mathrm{T}}(k, t) = \langle k \times j_k^{\mathrm{q}}(t) \cdot k \times j_k^{\mathrm{Q}}(0)^* \rangle \tag{6c}$$

and the longitudinal charge–charge current correlation

$$C_{\mathrm{QQ}}^{\mathrm{L}}(k, t) = \langle k \cdot j_k^{\mathrm{Q}}(t) k \cdot j_k^{\mathrm{Q}}(0)^* \rangle. \tag{6d}$$

These are then Fourier transformed, after smoothing with a Blackman window, to obtain the corresponding response functions in frequency space. The advantage of using these particular correlation functions, rather than the dynamic structure factor, is that they project out particular vibrational modes. The four correlation functions correspond, respectively, to the TA, LA, TO and LO modes. An example is shown in figure 6. Despite the high temperature, and consequent broadening of the responses, as well as statistical noise, the TA, LA and LO frequencies can be picked out with confidence, though the TO mode is somewhat problematical. The resulting dispersion curves in the [100] direction are shown in figure 7, where they are compared with LD calculations at the same volume. There are noticeable anharmonic frequency shifts.

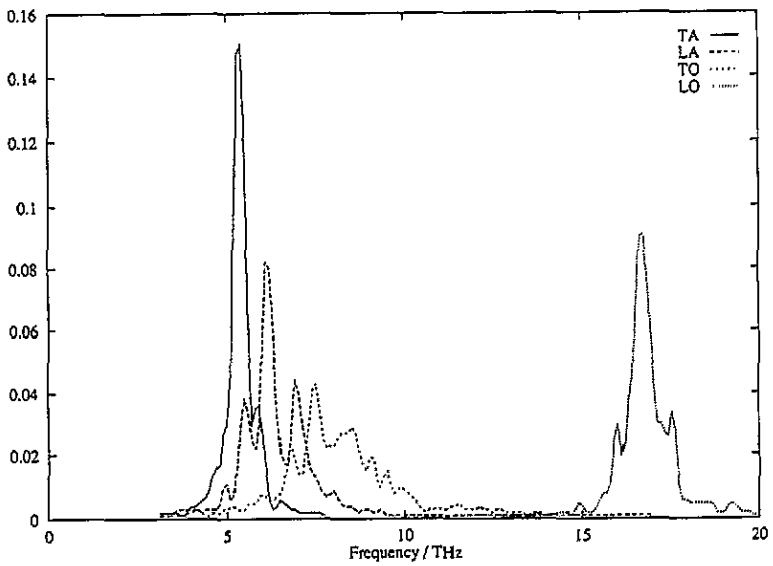

Figure 6. Fourier transforms of four current correlation functions defined in the text, at a temperature of 3000 K. The reciprocal space point is [0.4, 0, 0].

4. Conclusions

The method of quasi-harmonic lattice dynamics gives results for thermal expansion and internal energies in striking agreement with those from shell-model molecular-dynamics simulation, apart from expected zero-point effects, at temperatures up to 1500 K at atmospheric pressure, and up to higher temperatures at high pressure. Molecular-dynamics simulation has a particular utility at temperatures close to (and of course, above) the melting point where the quasi-harmonic method breaks down completely.

Both of the empirical potential models tested give thermal expansions that are too small compared with experiment, and high-pressure volumes that are too large. Prediction of properties under extreme conditions using potential models that are parameterized by fitting to data obtained under normal conditions is unlikely to be successful, and progress in this area will require the use of first-principles methods, or potential models fitted to first-principles results. Of the two models studied, the Lewis–Catlow model was better than

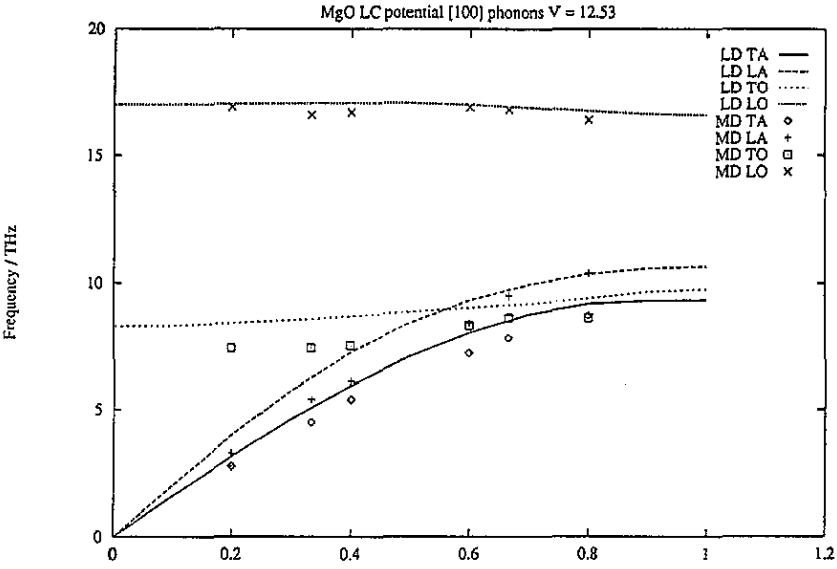

Figure 7. Phonon dispersion curves in the [100] direction, using the LC potentials. The MD results are from simulations at 3000 K; the LD results are at the same volume.

the Stoneham–Sangster model. (However, the latter model gives vibrational frequencies in better agreement with the experiment, since these frequencies were included in the fitting of the model parameters.)

The molecular-dynamics results show that the presence of ionic polarizability in a model has a noticeable effect on the thermal expansion, particularly at high pressure. It also, of course, has a dramatic effect on vibrational frequencies, and the results on the high-temperature solid demonstrate the utility of shell-model molecular-dynamics simulation in studying the details of the dynamics without any limitation to the harmonic regime.

Acknowledgments

We would like to thank ICI Chemicals and Polymers for provision of a post-doctoral fellowship for PJM. Computing facilities were provided by SERC through the Computational Science Initiative. We are grateful to M J Gillan, M Leslie and N L Allan for helpful discussions.

Appendix. Pressure calculations in the shell model

In order to perform the constant-pressure simulations described here we need a prescription for calculating the pressure when using the method of adiabatic dynamics to perform shell-model simulations. Since the internal degree of freedom of the ions is not in thermal equilibrium with the translational degrees of freedom, we prefer a mechanical starting point to a thermodynamic one. This is provided by the virial theorem, which for a system of N particles confined to a volume V by periodic boundaries takes the form [14]

$$pV = \tfrac{2}{3}\langle K\rangle + \tfrac{1}{3}\langle W\rangle \qquad \text{(A1)}$$

where K is the kinetic energy, and

$$W = \sum_{i<j} \boldsymbol{r}_{ij} \cdot \boldsymbol{f}_{ij}$$

is the virial. The $\sum_{i<j}$ indicates a sum over all pairs in the system, and, for short ranged forces, the pair separation $\boldsymbol{r}_{ij} = \boldsymbol{r}_i - \boldsymbol{r}_j$ is modified by the nearest-image transformation. In the case of Coulombic forces the Ewald sum is used; this is easy since the Coulombic energy is equal to the Coulombic virial. $\boldsymbol{f}_{ij}$ is the pair force exerted on particle i by particle j. The only ingredient entering the derivation of (A1) is classical mechanics, and the angular brackets represent time averages.

In the adiabatic shell model we can regard each ion as a 'molecule' containing two 'atoms', the core and the shell. We adopt this terminology since most of the following discussion can be equally well applied to polyatomic molecules. We adopt the notation whereby an italic index is used for a sum over molecules, and a greek index for a sum over atoms within a molecule.

There are two possible approaches we can adopt: we can apply the virial theorem to the molecules, ignoring their internal structure; or we can apply it to the atoms. In the molecule approach, we have

$$pV = \tfrac{2}{3}\langle K_C \rangle + \tfrac{1}{3}\langle W_C \rangle \tag{A2}$$

where K_C is the centre-of-mass kinetic energy, and W_C is the centre–centre virial

$$W_C = \sum_{i<j} \boldsymbol{R}_{ij} \cdot \boldsymbol{F}_{ij}$$

with $\boldsymbol{R}_{ij}$ being the separation between the centres of mass of the two molecules, and $\boldsymbol{F}_{ij}$ being the total pair force between the two molecules.

In the atom approach we must include all the kinetic energy in the system, including that in the internal degrees of freedom, and all the forces in the virial, including those from the bonds (the core–shell spring in our case). Then

$$pV = \tfrac{2}{3}\langle K_C \rangle + \tfrac{2}{3}\langle K_R \rangle + \tfrac{1}{3}\langle W_A \rangle + \tfrac{1}{3}\langle W_B \rangle. \tag{A3}$$

K_R is the kinetic energy of the internal degrees of freedom. W_A is the atom–atom virial

$$W_A = \sum_{i<j} \sum_{\alpha \text{in} i} \sum_{\beta \text{in} j} \boldsymbol{r}_{i\alpha j\beta} \cdot \boldsymbol{f}_{i\alpha j\beta}.$$

$\boldsymbol{r}_{i\alpha j\beta}$ is the separation between atoms on the two molecules, and $\boldsymbol{f}_{i\alpha j\beta}$ is the corresponding intermolecular atom–atom pair force. W_B is the bond virial

$$W_B = \sum_{i} \sum_{\alpha<\beta} \boldsymbol{r}_{i\alpha\beta} \cdot \boldsymbol{f}_{i\alpha\beta}^{\text{BOND}}.$$

The sum is over all bonds; in the shell-model case there is only one per molecule.

Of the two approaches, the molecule approach is conventionally taken in the simulation of small rigid molecules. This is because the use of the atom approach would require the inclusion of the constraint forces holding the bonds rigid, and these are not available if rigid-body equations of motion are being used. Our preference in the shell model is also to

use the molecule approach, on the grounds that the internal degree of freedom is a fictitious one introduced only to allow the ion to polarize.

In the molecule approach, the forces between molecules cannot be derived from a pair potential in the centre-of-mass coordinates, because the molecule has internal degrees of freedom whose coordinates affect the interaction between molecules. However, this does not mean that many-body terms are required in the molecule–molecule virial, since the total force on a molecule can be broken down into a sum of individual atom–atom forces. In fact, we have

$$F_{ij} = \sum_{\alpha \text{ in } i} \sum_{\beta \text{ in } j} f_{i\alpha j\beta}.$$

If we define

$$r_{i\alpha} = R_i + d_{i\alpha}$$

so that $d_{i\alpha}$ is the coordinate of atom α relative to the centre of mass of its molecule, and let

$$f_{i\alpha} = \sum_{j} \sum_{\beta \text{ in } j} f_{i\alpha j\beta}$$

be the total intermolecular force on atom α of molecule i, then with a little algebra we can express the centre–centre virial in terms of the atom–atom virial

$$W_C = W_A - \sum_{i} \sum_{\alpha \text{ in } i} d_{i\alpha} \cdot f_{i\alpha}. \tag{A4}$$

To calculate the pressure our procedure is to use this equation to calculate W_C, since this saves the necessity of calculating the centre–centre pair forces F_{ij} which are not otherwise required. This is then used in the molecule expression for the pressure, equation (A2).

Of course, the molecule approach and the atom approach must agree when ensemble averages are taken. We have previously verified this in the case of rigid molecules, when the constraint forces are included in the atom virial. In the case of the ideal (zero-shell-mass) shell model, it is possible to make a stronger statement: the two methods give identical *instantaneous* pressure. This can be seen as follows.

If the shell mass is zero we have $d_{ic} = 0$ and equation (A4) becomes

$$W_C = W_A - \sum_{i} d_{is} \cdot f_{is}$$

(c = core, s = shell). Substituting in (A2), the instantaneous pressure in the molecule approach is given by

$$pV = \tfrac{2}{3}K_C + \tfrac{1}{3}W_A - \tfrac{1}{3}\sum_{i} d_{is} \cdot f_{is}. \tag{A5}$$

In the atom approach the instantaneous pressure is given by

$$pV = \tfrac{2}{3}K_C + \tfrac{2}{3}K_R + \tfrac{1}{3}W_A + \tfrac{1}{3}\sum_{i} d_{is} \cdot f_{is}^{\text{BOND}} \tag{A6}$$

but K_R is zero since the shell has no mass. Also, in the zero-mass-shell model the shells relax instantaneously to zero-force positions, so that we must have

$$f_{is} = -f_{is}^{\text{BOND}}$$

and equations (A5) and (A6) become identical.

In our implementation of the shell model, the shells have some mass and are not necessarily exactly at zero force. Nevertheless we find that instantaneous values of pressure, as well as ensemble averages, are equal in the two approaches to an excellent degree of approximation.

References

[1] Catlow C R A and Mackrodt W C (ed) 1992 *Computer Simulation of Solids* (Berlin: Springer)
[2] Harrison N M and Leslie M 1992 *Mol. Simul.* **9** 171
[3] Gale J D, Catlow C R A and Mackrodt W M 1992 *Modelling Simul. Mater. Sci. Eng.* **1** 73
[4] Dick B G and Overhauser A W 1958 *Phys. Rev.* **112** 90
[5] Allan N L, Braithwaite M, Cooper D L, Mackrodt W C and Wright S C 1991 *J. Chem. Phys.* **95** 6792
[6] Allan N L, Mackrodt W C and Leslie M 1987 *Adv. Ceramics* **23** 257
[7] Matsui M 1989 *J. Chem. Phys.* **91** 489
[8] Mitchell P J and Fincham D 1993 *J. Phys.: Condens. Matter* **5** 1031
[9] Stoneham A M and Sangster M J L 1985 *Phil. Mag.* B **52** 717
[10] Lewis G V and Catlow C R A 1985 *J. Phys. C: Solid State Phys.* **18** 1149
[11] Fincham D 1993 *J. Mol. Graphics* at press
[12] Anderson O L and Zou K 1990 *J. Phys. Chem. Ref. Data* **19** 69, quoting experimental data from Suzuki I 1975 *Phys. Chem. Earth* **23** 145
[13] Mao H K and Bell P M 1979 *J. Geophys. Res.* **84** 4533
[14] Haile J M 1992 *Molecular Dynamics Simulation* (New York: Wiley) appendix B